

Fragment-Based Deconstruction of Bcl-x_L Inhibitors

Sarah Barelier,[†] Julien Pons,[†] Olivier Marcillat,[‡] Jean-Marc Lancelin,[†] and Isabelle Krimm^{*,†}

[†]Laboratoire des Sciences Analytiques, UMR CNRS 5180, Université de Lyon, Université Claude Bernard, Lyon 1, Bât. ESCPE Lyon, Domaine Scientifique de la Doua, 69100 Villeurbanne, France, and [‡]ICBMS, UMR5246, Université de Lyon, Université Claude Bernard, Lyon 1, Domaine Scientifique de la Doua, 43 Boulevard du 11 Novembre 1918, 69100 Villeurbanne, France

Received January 6, 2010

Fragment-based drug design consists of screening low-molecular-weight compounds in order to identify low-affinity ligands that are then modified or linked to yield potent inhibitors. The method thus attempts to build bioactive molecules in a modular way and relies on the hypothesis that the fragment binding mode will be conserved upon elaboration of the active molecule. If the inverse process is considered, do the fragments resulting from the deconstruction of high-affinity inhibitors recapitulate their binding mode in the large molecule? Few studies deal with this issue. Here, we report the analysis of 22 fragments resulting from the dissection of 9 inhibitors of the antiapoptotic protein Bcl-x_L. To determine if the fragments retained affinity toward the protein and identify their binding site, ligand-observed and protein-observed NMR experiments were used. The analysis of the fragments behavior illustrates the complexity of low-affinity protein–ligand interactions involved in the fragment-based construction of bioactive molecules.

Introduction

Fragment-based drug design has developed significantly over the past 10 years and is now recognized as a successful method of hit identification and lead conception.¹ The method was proposed by Abbot in 1996 and has gained more and more interest in the following years to finally become a tangible alternative to high-throughput screening.^{2,3} Fragment-based drug discovery programs are now routinely used in most pharmaceutical companies and have already yielded very promising results.⁴ The method consists of screening a small set (typically several hundreds to several thousands) of low molecular weight (< 300 Da) compounds, called the fragments. Because of their low complexity, the fragments usually display low affinity for the target protein, but optimization of the fragment hits, usually by addition of new chemical functions or alternatively by linking of two fragment hits binding in adjacent pockets, can provide very potent lead compounds, as largely demonstrated in the literature.^{1,3,5,6}

This method of lead conception relies on the premise that the binding site and binding mode of the fragments are conserved upon modification of the fragments and that when two fragments are linked together, their orientation in their respective binding pockets should remain the same. Moreover, each modification of the molecule, for example, by addition of a substituent or by linkage of a new fragment to the molecule, is supposed to either increase its ligand efficiency (binding energy divided by the number of heavy atoms) or at least keep it constant.^{7,8} Hence, the ideal lead compound would be a molecule constituted of small fragments linked together, each of them keeping the same position and orientation on the protein whether they are alone or part of the bigger lead compound.

Much has been discussed about the contributions of the different fragments of a bioactive molecule to the binding energy and affinity for the target; however, very few practical examples have been published in the literature.^{9,10} Hadjuk et al. published an interesting retrospective analysis of 18 drug leads that were reduced in size until the smallest compound retaining potency for the target protein was identified.⁸ The affinities of the different subcompounds were measured, and the study highlighted a nearly linear relationship between potency and molecular weight. On the other hand, Babaoglu et al. presented the deconstruction of a known β -lactamase inhibitor into three fragments and showed that none of them bound in a position that recapitulated its placement in the larger inhibitor.¹¹ In fact, the fragments bound to previously unexplored binding sites at the surface of the protein, and it is only by increasing the complexity of one of the fragments that its original binding site and orientation could be restored. In another study,¹² the natural cyclopentapeptide argifin, a chitinase inhibitor, was dissected into four linear peptides and the dimethylguanyllurea molecule. The peptides and the dimethylguanyllurea molecule were analyzed by X-ray crystallography, and their conformations were shown to be remarkably similar to that of the natural product.

Hence, the question of the binding conservation upon defragmentation of a molecule is still unclear. When an inhibitor is defragmented into smaller pieces, do the fragments still display affinity for the target, and if so, do they keep their initial binding site on the macromolecule? To address this question, we present here the first study of the deconstruction of nine inhibitors targeting the same macromolecule, the well-characterized antiapoptotic protein Bcl-x_L. Bcl-x_L belongs to the Bcl-2 family of proteins that is involved in the mitochondrial pathway of apoptosis.^{13,14} Several proteins within this family, including Bcl-x_L, inhibit programmed cell death, while others, such as Bax and Bak, can promote apoptosis.

*To whom correspondence should be addressed. Phone: 0033 472 431 825. Fax: +33-472431395. E-mail: isabelle.krimm@univ-lyon1.fr.

Interactions between these two groups of proteins antagonize their different functions and modulate the sensitivity of a cell to apoptosis.^{15,16} Hence, these proteins have been shown to be attractive therapeutic targets for the treatment of cancer.¹⁷ In vivo, several proapoptotic proteins counteract the antiapoptotic action of Bcl-x_L by binding to a shallow groove on the surface of the protein, also referred to as the binding cleft region.^{14,18} Several small molecules targeting the binding cleft of Bcl-x_L and competing with its natural proapoptotic partners have been published in the literature; among them some are currently in clinical phase.^{19–28}

In the study reported here, nine inhibitors of Bcl-x_L have been selected and dissected into small commercially available compounds with sizes ranging from 101 to 277 Da. Each fragment was tested by 1D ligand-observed NMR^a experiments to determine if it retained affinity toward the target protein or not. For the fragments that were identified as ligands, the binding site was determined from protein-observed nuclear magnetic resonance (NMR) experiments. Derivatives of several fragments were then tested to confirm our results and to assess the effect of small chemical modifications on binding to the target protein. This study, which investigates for the first time the behavior of a series of fragments obtained from different inhibitors of the same protein, shows that the fragment molecules can (1) exhibit no detectable affinity for the protein, (2) bind to the protein in a similar position as in the lead they come from, or (3) bind to the protein in binding sites different from the original lead. Hence, the work reported here provides new insights into the complexity of low-affinity protein–ligand interactions.

Results

Deconstruction of the Inhibitors of the Bcl-2 Family of Proteins into Fragments. The inhibitors of Bcl-x_L selected for this study are displayed in Table 1: **1** (((*R*)-4-(3-morpholin-4-yl-1-phenylsulfanylmethyl)propylamino)-*N*-(4-{4-[2-(4-chlorophenyl)-5,5-dimethylcyclohex-1-enylmethyl]piperazin-1-yl}benzoyl)-3-trifluoromethanesulfonylbenzenesulfonamide), also known as ABT-263 and **2** (*N*-(4-[4-(4-chlorobiphenyl-2-ylmethyl)piperazin-1-yl]benzoyl)-4-(3-dimethylamino-1-phenylsulfanylmethylpropylamino)-3-nitrobenzenesulfonamide, also known as ABT-737) from Abbott Laboratories are the results of a fragment-based drug design program targeting the antiapoptotic Bcl-2 family of proteins.^{22,27} **3** (3-iodo-5-chloro-*N*-[2-chloro-5-((4-chlorophenyl)sulfonyl)phenyl]-2-hydroxybenzamide, also known as BH3I-2) was discovered during a high-throughput screening based on fluorescence polarization and was shown to disrupt the interaction between Bcl-x_L and the Bcl2 homology domains 3 (BH3) of Bak;¹⁹ **4** (4-(1,3-benzodioxol-5-yl)-6-(2-hydroxyphenyl)-2-oxo-1,2-dihydropyridine-3-carbonitrile, also known as BI21-C5) and **5** (2-{4-[(4-chlorophenyl)thio]-3-nitrobenzoyl}benzoic acid, also known as BI21-C6) come from a drug discovery project based on molecular docking and NMR screening;²⁵ **6** ((–)-gossypol) is a natural polyphenol contained in green tea displaying inhibitory activity toward different members of the Bcl-2 family of

proteins including Bcl-x_L;²⁹ **7** (2-[2-[(3,5-dimethyl-1*H*-pyrrol-2-yl)methylene]-3-methoxy-2*H*-pyrrol-5-yl]-1*H*-indole methanesulfonate, also known as obatoclax) is an indole-derivative small molecule inhibitor of Bcl-2 proteins;²¹ **8** (2-((2*S*,3*R*,4*S*)-4-biphenyl-4-ylcarboxamido-1-(biphenyl-carbonyl)-3-hydroxy-6-((2-methoxyethoxy)methoxy)-1,2,3,4-tetrahydroquinolin-2-yl)acetic acid, also known as mipralden) results from the screening of a tetrahydroaminoquinoline-based library and binds to both Bcl-x_L and Mcl-1;²³ **9** (*N*-[(2-*tert*-butylbenzenesulfonyl)phenyl]-2,3,4-trihydroxy-5-(2-isopropylbenzyl)benzamide, also known as TW-37) is a benzenesulfonyl derivative initially designed to inhibit Bcl-2 that also displays affinity for Bcl-x_L and Mcl-1.²⁰

The inhibitors were deconstructed into two to six fragments as illustrated in Table 2, yielding 22 fragments. The small commercially available molecules contain at least one five-/six-atom ring, with a molecular weight between 101 and 277 Da.

Ligand-Observed NMR Assay of the Fragments Binding to Bcl-x_L. The 22 fragments were tested for binding to Bcl-x_L by 1D NMR. First, 1D and Water–Ligand Observed via Gradient Spectroscopy (WaterLOGSY) spectra were recorded to check the solubility and stability of the fragments in the protein buffer. Then WaterLOGSY^{30,31} and saturation transfer difference (STD)³² experiments were performed in presence of the protein (Figure 1). The results are summarized in Table 2. As shown, 19 out of 22 fragments display 1D NMR spectra that indicate that they interact with Bcl-x_L whereas no binding was detected for the three remaining fragments (**13** (sulfanilamide), **14** (4-methylmorpholine), and **19** (3-cyano-6-methyl-2-pyridinone)). For the 19 hit fragments, the binding was demonstrated by both WaterLOGSY and STD experiments (Figure 1). To confirm the binding and to rank the ligands of Bcl-x_L, the STD factors (*f*_{STD}) of the fragments were measured (Figure 2).³³ As reported in Table 2, the *f*_{STD} values strongly vary from one fragment to another, ranging from 4 to 100. However, no clear correlation is observed between the fragment properties (molecular weight, number of cycles, number of heteroatoms, number of donors or acceptors of hydrogen bonds) and the *f*_{STD} values reported for the fragments.

Protein-Observed NMR Assay of the Fragments Binding to Bcl-x_L. All the fragments were further analyzed through protein-observed experiments. ¹H–¹⁵N heteronuclear single quantum correlation (¹H–¹⁵N HSQC) experiments were recorded in the absence and in the presence of the fragments, and changes in the spectra of the Bcl-x_L protein were monitored. As expected, the three fragments determined as non-ligand by 1D NMR experiments (**13**, **14**, and **19**) did not induce chemical-shift variations on the 2D spectra. Moreover, for six other fragments (**11** (1-benzylpiperazine), **12** (2-piperazin-1-ylaniline), **15** (sulfabenzamide), **16** (benzanilide), **27** (1-benzoylpiperidine), and **29** (4-benzamidopiperidine)), no chemical-shift perturbations were observed on the HSQC spectra upon fragment addition (2 mM) to the protein. The remaining fragments (**10** (2-phenylphenol), **17** (diphenylsulfone), **18** (1,3-benzodioxole), **20** (2-benzoylbenzoic acid), **21** (2-phenylthioaniline), **22** (2,3-dihydroxynaphthalene), **23** (1,7-dihydroxynaphthalene), **24** (indole), **25** (2-((3,5-dimethyl-2*H*-pyrrol-2-ylidene)methyl)-3,5-dimethyl-1*H*-pyrrole monohydrochloride), **26** (1,2,3,4-tetrahydroquinoline), **28** (4-biphenylcarboxamide), **30** (bis(2-hydroxyphenyl)methane), and **31** (2,3,4-trihydroxybenzophenone)) were shown to induce significant chemical-shift

^a Abbreviations: BH3, Bcl2 homology domains 3; EDTA, ethylenediaminetetraacetic acid; HAC, heavy atom count; HSQC, heteronuclear single quantum coherence; LGA, Lamarckian genetic algorithm; NMR, nuclear magnetic resonance; NOESY, nuclear Overhauser effect spectroscopy; PDB, Protein Data Bank; STD, saturation transfer difference; WaterLOGSY, water–ligand observed via gradient spectroscopy.

Table 1. Bcl-x_L Inhibitors Selected for Defragmentation: Name, Structure, Published Affinity or Activity toward Bcl-x_L, Molecular Weight (MW)

Inhibitor	Structure	Activity	Molecular Weight (Da)	Reference
1 (ABT-263)		K _i < 1 nM	975	27
2 (ABT-737)		IC ₅₀ 64 nM	847	22
3 (BH3I-2)		K _D 4.1 μM	536	19
4 (BI21-C5)		IC ₅₀ 5.1 μM	332	25
5 (BI21-C6)		IC ₅₀ 0.5 μM	415	25
6 ((-)-Gossypol)		IC ₅₀ 480 nM	547	24
7 (Obatoclax)		IC ₅₀ 4.69 μM	317	21
8 (Mipralden)		K _D 70 μM	597	23
9 (TW-37)		K _i 1.11 μM	574	20

Table 2. Fragments Resulting from the Deconstruction of the Bcl-x_L Inhibitors^a

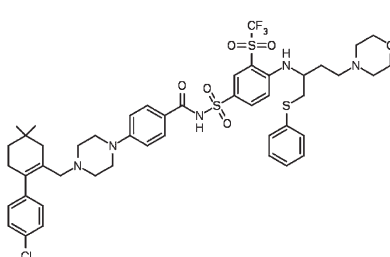
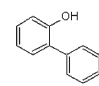
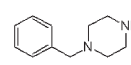
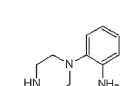
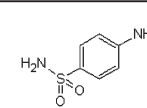
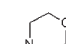
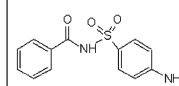
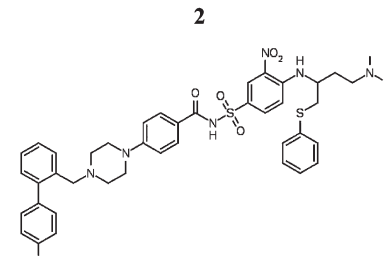
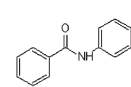
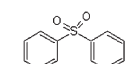
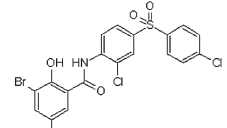
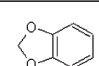
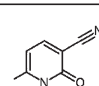
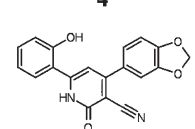
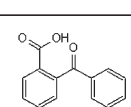
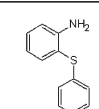
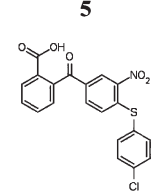
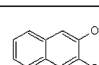
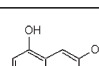
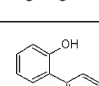
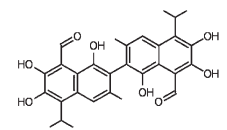
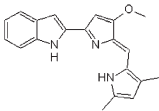
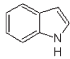
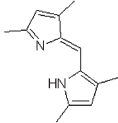
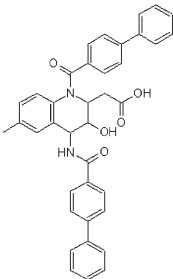
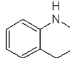
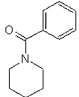
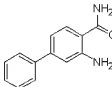
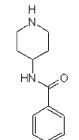
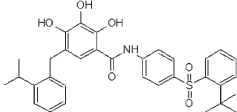
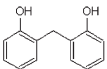
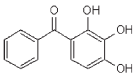
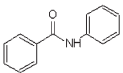
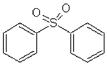
Inhibitor	Fragments			1D NMR	f_{STD}	2D NMR
	Molecule name	MW (Da)	Chemical structure			
1 	10	170.21		Binding	92	Site 1
	11	176.26		Binding	12	No $\Delta\delta$
	12	177.25		Binding	20	No $\Delta\delta$
	13	171.28		No	0	No $\Delta\delta$
	14	101.15		No	0	No $\Delta\delta$
	15	276.31		Binding	4	No $\Delta\delta$
2 	16	197.23		Binding	16	No $\Delta\delta$
	17	218.27		Binding	44	Site 1
3 	18	122.12		Binding	36	Site 1
	19	138.17		No	0	No $\Delta\delta$
4 	20	226.23		Binding	12	Site 1
	21	201.29		Binding	20	Site 1
5 	22	160.17		Binding	64	Site 1
	23	160.17		Binding	48	Site 1
	10	170.21		Binding	92	Site 1
6 						

Table 2. Continued

Inhibitor	Fragments			1D NMR	f_{STD}	2D NMR
	Molecule name	MW (Da)	Chemical structure			
7 	24	117.15		Binding	56	Site 1
	25	200.28		Binding	100	Site 1 + Other binding sites
8 	26	133.19		Binding	36	Site 1
	27	189.25		Binding	20	No $\Delta\delta$
	28	212.25		Binding	n.a.	Site 1
	29	204.27		Binding	4	No $\Delta\delta$
9 	30	200.24		Binding	72	Site 1
	31	230.22		Binding	80	Site 1
	16	197.23		Binding	16	No $\Delta\delta$
	17	218.27		Binding	44	Site 1

^a The fragments were tested for binding by 1D NMR (STD and WaterLOGSY experiments). For each fragment, the STD factor (f_{STD}) was determined. The fragments were then tested by 2D protein-observed NMR (^{15}N -HSQC) and the binding site was determined by chemical shift mapping.

perturbations on the protein spectrum (Figure 3). As shown in Table 2, all the fragments that do not induce any perturbation on the protein NMR spectrum exhibit STD factors lower than 20. This suggests that these fragments are not detected as ligands in the HSQC experiments because of a too weak binding affinity and/or nonspecific binding. Indeed, 1D NMR methods such as WaterLOGSY or STD allow one to detect fragment–protein interactions even when working at a concentration much lower than the K_D value and are thus more sensitive than the methods based on the observation of chemical shift changes such as 2D ^{15}N -HSQC. WaterLOGSY and

STD thus identify fragments with binding affinities too low to induce chemical shifts changes on the protein spectrum. For the hit fragments exhibiting chemical shift changes in the 2D experiments, a good correlation is observed between the f_{STD} value and the strength of the chemical shifts induced by addition of the fragment to the protein.

Binding Site of the Fragments. To go further into the characterization of the binding sites of the fragments, the backbone resonances of Bcl-x_L have been assigned using triple-resonance NMR experiments (HN(CO)CA, HNCA, HNCACB) and a ^{15}N -nuclear Overhauser effect spectroscopy

HSQC (^{15}N -NOESY-HSQC) experiment. For one fragment (**25**), the $^1\text{H}^{\text{N}}$ and ^{15}N chemical shift changes are scattered into different regions on the protein surface, suggesting that **25** binds to several different sites. For the other 12

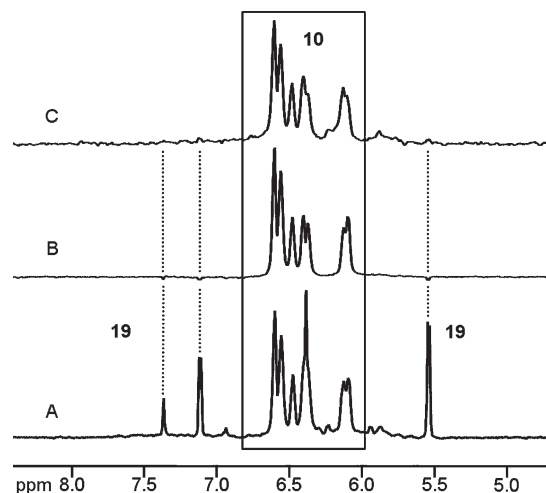


Figure 1. 1D ligand-observed NMR experiments recorded on the Bcl-x_L protein: (A) 1D spectrum, (B) WaterLOGSY spectrum, and (C) STD spectrum of fragments **10** and **19**. Fragment **10** binds to Bcl-x_L, as illustrated by the STD and WaterLOGSY spectra, whereas **19** does not interact with the protein.

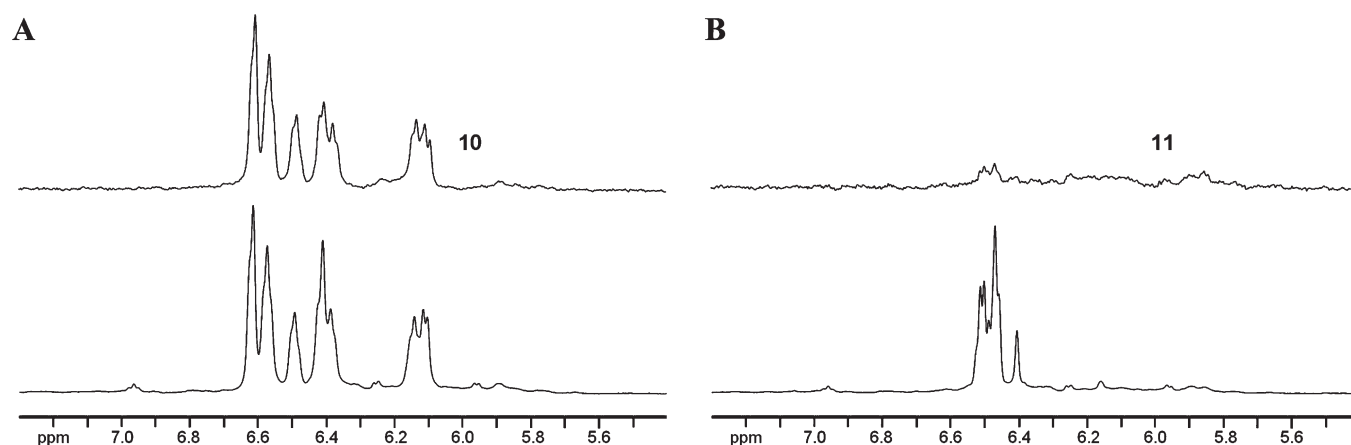


Figure 2. Measurement of the f_{STD} value for fragments **10** and **11**. STD spectra and 1D spectra are displayed in the upper panel and lower panel, respectively: (A) fragment **10**; (B) fragment **11**.

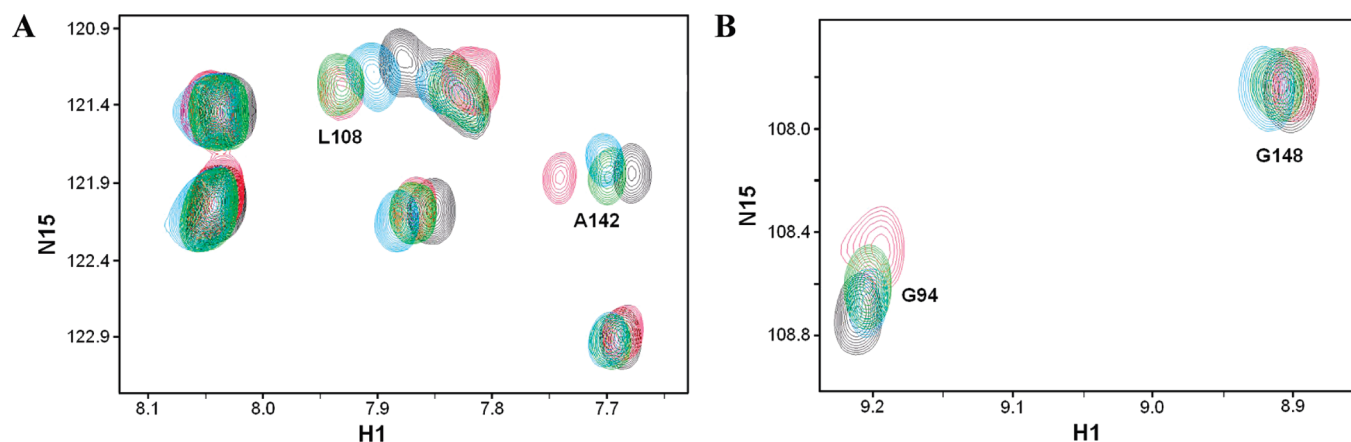


Figure 3. Superposition of the 2D ^{15}N -HSQC spectra of Bcl-x_L recorded at 28 °C in the absence and in the presence of fragments **10** (red), **20** (cyan), and **30** (green). The reference spectrum is displayed in black.

fragments (**10**, **17**, **18**, **20**, **21**, **22**, **23**, **24**, **26**, **28**, **30**, and **31**), the chemical shifts perturbations involve amino acids localized within the same region on the protein surface (Figure 4). These perturbed amino acids belong to helix α_2 (L90, G94, D95, F97, E98), the loop between helices α_2 and α_3 (L99, R100, Y101, R102, R103), helix α_3 (A104, F105, S106, L108, S110, L112), helix α_4 (E129, L130, F131, R132, D133, G134), and helix α_5 (W137, G138, R139, A142, F143, S145, F146, G147, A149). The most important changes are observed for residues F97, E98, Y101, R102, F105, S106, and A142. Hence, the NMR data clearly show that the fragments **10**, **17**, **18**, **20**, **21**, **22**, **23**, **24**, **26**, **28**, **30**, and **31** resulting from the different inhibitors all bind into the same site. Figure 4 shows **10** docked to Bcl-x_L within the pocket defined by the experimentally observed chemical shifts. This binding site corresponds to the pocket occupied by L578 and I581 of the Bak peptide in the Bcl-x_L/Bak complex¹⁸ (Protein Data Bank (PDB) code 1BXL) and also corresponds to the binding site of the fluorobiphenyl acid molecule from which inhibitor **2** was designed.³⁴ The binding pose of lowest energy, which corresponds to a cluster containing 70% of the 50 docked structures, is displayed.

Affinity of the Fragments. The binding constant of **10**, which is the best site 1 ligand in terms of f_{STD} , was determined by monitoring the changes in protein chemical shift upon titration with the fragment (Figure S1 in Supporting Information). **10** binds to Bcl-x_L with a 2.7 ± 0.5 mM affinity. According to the f_{STD} measurements, all other

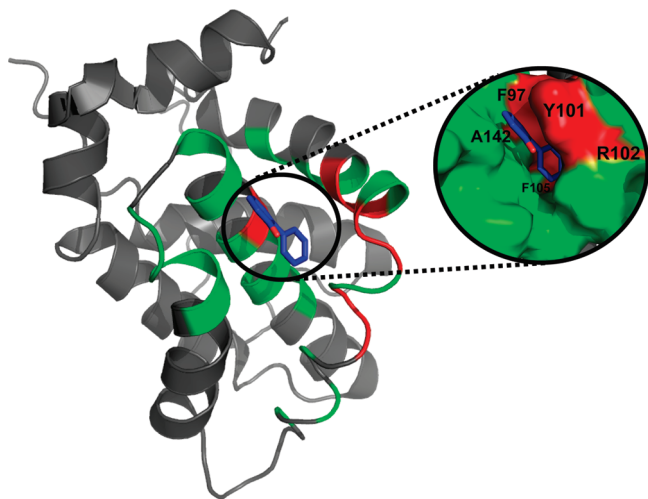


Figure 4. Identification of the binding region of the fragments on the 3D structure of Bcl-x_L (PDB entry 1YSG). The chemical shift variations are mapped on the 3D structure of the protein and colored in green and red for the weak and strong perturbations, respectively. Fragment **10**, docked with the AutoDock4 program, is displayed as blue sticks.

fragments (except **25**) are weaker binders than **10**. However, because of their low affinity and their poor solubility in water, it was not possible to obtain reliable measurements and to determine their binding constant, which likely lies in the low millimolar range.

NMR Study of Fragment Analogues. Analogues of the fragments were also studied by NMR experiments to confirm our observations and explore the impact of functional group addition or substitution (Table 3). First, analogues of fragments **11**, **12**, **13** (inhibitor **2**), and **16** (inhibitors **3** and **9**) that were shown not to bind Bcl-x_L or to be very weak ligands ($f_{STD} < 20$) were analyzed. A methyl group and an ethanamine group were added to **11** to yield **32** ((2-((4-methylpiperazin-1-yl)methyl)phenyl)methylamine), and **12** was modified by replacing the amine moiety by a methoxy group (**33** (1-(3-methoxyphenyl)piperazine)) or by an alcohol function (**34** (1-(4-hydroxyphenyl)piperazine)). The amine moiety of **13** was removed (**35** (benzenesulfonamide)) or replaced in another compound by a methyl group with the sulfonamide group extended into a sulfonylacetamide group (**36** (sulfacetamide)). Finally, **16** was modified by addition of amine moieties to the benzyl rings (**37** (4,4'-diaminobenzanilide)). No binding or very weak binding was observed for the derivatives of **11**, **12**, **13**, and **16**, with f_{STD} values varying from 0 to 16.

Then analogues of fragments that were detected as ligands of Bcl-x_L in both the 1D NMR spectra and the protein HSQC spectra were analyzed. **20** (from inhibitor **5**) was modified by replacement of the carboxylic function by two alcohol functions (**38** (2,4-dihydroxybenzophenone)). **38** induced larger chemical shift perturbations than **20** in the 2D NMR experiments, in agreement with the large increase of the f_{STD} value from fragment **20** ($f_{STD} = 12$) to its analogue **38** ($f_{STD} = 92$). Derivatives of **22/23** (from inhibitor **6**) and **10** (**2**, **6**) were also tested for binding. One hydroxyl function of **23** was moved to the next carbon atom (**39** (2,7-dihydroxynaphthalene)), which had a poor effect on binding to Bcl-x_L. Similarly, variation of the position of hydroxyl functions on fragment **10** did not strongly change the f_{STD} value, as shown in Table 3, and the addition of a methoxy group (**42**

(6-methoxy-1*H*-indole)) to the pyrrole ring of **24** did not modify the molecule binding. Finally, fragments **30** and **31** from inhibitor **9** were also modified. One hydroxyl function of **30** was removed and the other one was modified into a methanol moiety to yield **43** (2-benzylbenzyl alcohol), which appeared as a weaker ligand than **30**. **31** was modified by deleting or moving the hydroxyl functions on the benzyl rings (**44** (2,4,4'-trihydroxybenzophenone), **38**). Both **44** and **38** displayed f_{STD} values similar to that of **31**. These results thus show that the derivatives mostly behave like the original fragment (except **20/38**) and indicate that the small chemical modifications do not strongly modify the binding properties of the fragments (Table 3). The small size and the low complexity of the fragments may account for the tolerance observed, as well as the fact that the binding site on the protein surface is fairly large.

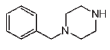
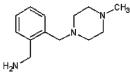
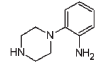
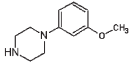
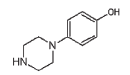
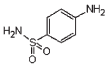
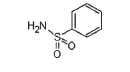
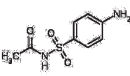
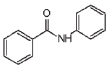
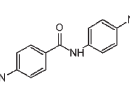
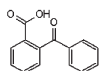
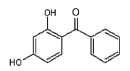
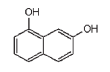
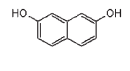
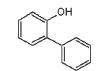
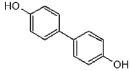
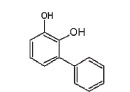
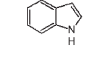
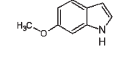
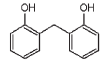
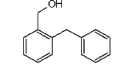
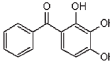
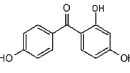
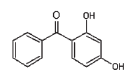
Discussion

In this work, nine inhibitors of the Bcl-x_L protein were deconstructed into fragment molecules in order to study how the fragments behave when they are detached from the initial molecule. 1D and 2D NMR experiments were used to probe the interactions of the small molecules with the protein and to determine whether the fragments were able to retain affinity for the protein or not and if the binding site of the fragments was conserved after defragmentation. In the dissection process of the inhibitors, the fragments were chosen on the basis of their resemblance to the initial lead, their small size (< 300 Da), their solubility properties, and their commercial availability. The fragments should be as simple as possible, with respect to the fragment rule of three.³⁵ As shown in Table 2, each inhibitor was defragmented into two to six fragments, with a total of 22 fragments obtained from the nine inhibitors. Only three fragments are found in more than one inhibitor (**10** is common to inhibitors **2** and **6**, and **16** and **17** are fragments of **3** and **9**). The binding of the fragments to the Bcl-x_L protein was investigated by ligand-observed and protein-observed NMR experiments (Table 2, Figures 1, 2, and 3). To confirm our observations and explore the impact of functional group addition or substitution, several derivatives of the fragments were also studied (Table 3). This work reveals that the fragments can display very different behaviors.

The first observation is that 9 out of the 22 fragments were shown not to bind Bcl-x_L or to be very weak ligands of the protein. Among them, three fragments (**13**, **14**, and **19**) did not induce a signal in the 1D NMR binding experiments. As shown in Table 2, these three fragments contain only one six-atom ring and are likely not complex enough to retain affinity for the protein. The second group is composed of six fragments identified as very weak ligands ($f_{STD} < 20$ and no perturbations in the protein-observed experiments). Considering the number of rings, heavy atoms, heteroatoms, or functional groups, these six fragments (**11**, **12**, **15**, **16**, **27**, and **29**) do not appear less complex than the fragments that display a greater affinity for the protein (see **24** or **26**). So why did these molecules not retain affinity for Bcl-x_L?

In the cases of fragments **27** and **29** from inhibitor **8**, the results we observe likely reflect the fact that the defragmentation enables one to identify the fragments that appear to be responsible for forming most of the key interactions in the inhibitor–protein complex. The dissection analysis clearly shows that the tetrahydroquinoline (**26**) and the biphenylcarboxamide (**28**) represent efficient binders and attractive starting points for structure based optimization, compared to

Table 3. NMR Analysis of 10 Fragments Resulting from Bcl-x_L Inhibitors^a

Fragments			Analogues			
Molecule	Structure	f_{STD}	Molecule	Structure	f_{STD}	Binding site
11		12	32		4	No $\Delta\delta$
12		20	33		16	No $\Delta\delta$
			34		12	No $\Delta\delta$
13		0	35		4	No $\Delta\delta$
			36		0	No $\Delta\delta$
16		16	37		4	No $\Delta\delta$
20		12	38		92	Site 1
23		48	39		40	Site 1
10		92	40		60	Site 1
			41		52	Site 1
24		56	42		52	Site 1
30		72	43		28	Site 1
31		80	44		72	Site 1
			38		92	Site 1

^aFor each derivative, the STD factor (f_{STD}) was determined and the binding site was assessed using protein-observed 2D NMR experiments (¹⁵N HSQC).

fragments **27** and **29**. On the other hand, fragment **16**, present in inhibitors **3** and **9**, has a level of complexity similar to good ligands such as **24** or **26** but lacks the specificity determinants of the original inhibitors it results from (**3**, **9**). Hence, fragment **16** does not retain affinity for the protein, mostly behaving as a linker in the original inhibitor.

The three others fragments **11**, **12**, and **15** that are not able to bind Bcl-x_L belong to inhibitor **2**. Notably, four of the five fragments resulting from the dissection of **2** are not efficient binders (Table 2). These results were confirmed by the study of derivatives of **11**, **12**, and **13** (see Table 3). Here, the absence of binding is not due to a loss of complexity of the fragment compared to the fragment included in the inhibitor. The loss of affinity is more likely related to the emergent binding mode of the large inhibitor **2** (847 Da). The 3D structure of the **2**/Bcl-x_L complex shows that the binding of the large inhibitor induces conformational changes in the interaction region (PDB entry 2YXJ).²² The fragments of **2** are not able to induce such conformational changes, and the affinity is therefore not conserved. However, the case of small molecules being able to induce new binding sites was recently reported for fragments resulting from the β -lactamase inhibitor,¹¹ where new sites for ligand interaction were observed upon binding of the fragments.

Another important observation concerns the binding site of the fragments. Thirteen fragments were shown to display significant chemical shift perturbations on the Bcl-x_L NMR spectrum, and their binding site was characterized by chemical-shift mapping on the protein surface (Figures 3 and 4). As illustrated in Figure 4, the fragments **10**, **17**, **18**, **20**, **21**, **22**, **23**, **24**, **26**, **28**, **30**, **31** all induce perturbations of residues located in the same pocket that is targeted by the initial inhibitors (namely, helix α 2, the loop between helices α 2 and α 3, helix α 3, helix α 4, and helix α 5). Only **25** is shown to bind Bcl-x_L at different binding sites. More precisely, all the fragments except **25** bind in a pocket that corresponds to the binding site of the fluorobiaryl acid (from inhibitor **2**) and is referred to as site 1 in previous studies (Figure 4).³⁴ Our work shows that even if the fragments bind in the same overall region as the initial inhibitors, they do not necessarily retain the exact position they had in the lead they were extracted from. For instance, the comparison of the Bcl-x_L/**2** structure with the chemical shifts induced by **10** clearly shows that the position of the fragment is shifted and that the fragment does not bind in the same position whether it is alone or part of the inhibitor (Figure 5).³⁶ In the model proposed for the Bcl-x_L/**6** complex, the first naphthalene moiety mainly interacts with F97, R100, Y101, V126, E129, L130, R139 and the second one with F97, R100, E96, Y195, A200.^{37,38} From our results, it appears that the preferred binding site for the naphthalene fragments (**22**, **23**) corresponds to the binding site of the first moiety only. Again, according to the model proposed for the Bcl-x_L/**5** complex, the inhibitor spans between site 1 and site 2.²⁵ Hence, fragments **20** and **21** would be expected to bind to sites 1 and 2, respectively, whereas chemical shift mapping shows that both of them bind to site 1. Finally, in the model proposed for the Bcl-x_L/**8** complex, the two biphenyl moieties extend into sites 1 and 2, with the quinoline linker lying close to helix α 6. However, in our study, we find that the fragments of **8** preferably bind into site 1 only, instead of retaining their initial position in the inhibitor. The same conclusions can be drawn regarding inhibitors **7** and **9**, for which models of the Bcl-2/inhibitor complexes were proposed.^{21,39} A particular behavior is observed for fragment **25** (inhibitor **7**), which

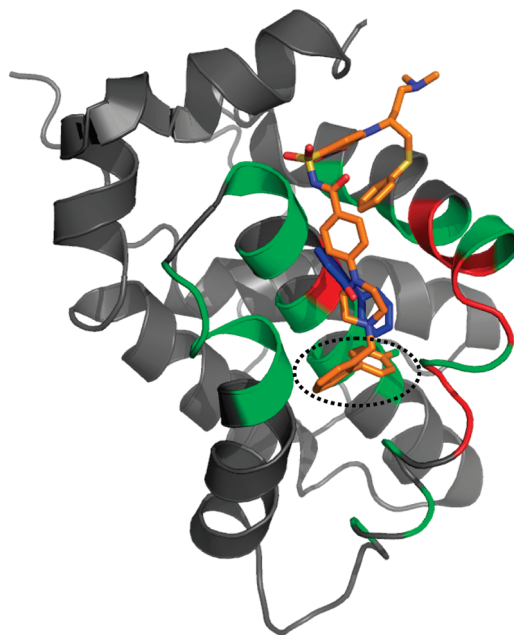


Figure 5. Superposition of **10** (blue sticks) and the original inhibitor **2** (orange sticks) on the structure of Bcl-x_L (PDB entry 2YXJ). The position of the biphenyl moiety within **2** is circled by a black dotted line.

displays several binding sites on the protein surface. In spite of the complexity of the molecule, the fragment requires that it be included in the whole inhibitor to interact specifically in the Bcl-x_L binding cleft region. All these observations show that the emergent binding mode of large molecules makes the fragment-based constructive approach more complex by challenging the binding mode prediction of elaborated inhibitors.

The last question deals with the conservation of the ligand efficiency (LE) from the fragment to the inhibitor. To address this issue, the binding affinity of **10**, which displays the highest f_{STD} among all site 1 ligands, was determined. All other fragments (except **25**) are thus expected to bind to Bcl-x_L with a lower affinity than **10** (2.7 ± 0.5 mM). Following Hadjuk's observation that ligand efficiency should ideally remain constant during the hit-to-lead optimization process,⁸ one can calculate the minimal affinity that each fragment should display in order to exhibit a ligand efficiency at least as high as the ligand efficiency of the original inhibitor (Table 4). For **10** for instance, a minimal affinity of 4.8 mM is required for the fragment to display a 0.25 ligand efficiency. Thus, this fragment, with a 2.7 mM affinity, can be considered as an efficient binder, or in other words, **10** possesses a high group efficiency within inhibitor **2**.⁴⁰ The same conclusion can be drawn for **26** and **28** from inhibitor **8**: given the chemical shifts induced on the protein spectrum, **26** and **28** likely bind to Bcl-x_L with better affinities than needed for a 0.13 ligand efficiency (119.3 and 33.3 mM, respectively) and thus provide high group efficiency in molecule **8**. On the other hand, several fragments such as **15**, **16**, **17**, **20**, or **21** would need to display affinities lower than 2.0 mM in order to possess the same ligand efficiency as the inhibitor they come from, which is not the case according to the f_{STD} measurements and chemical shifts observations. So these fragments probably display a low group efficiency and might be replaced by more efficient binders in the inhibitor.

Three others studies that explored the structural properties of fragments resulting from a larger inhibitor or substrate

Table 4. Expected K_D and LE of the Fragments Resulting from the Dissection of Bcl-x_L Inhibitors^a

inhibitor (LE)	fragment		expected K_D (mM)
	molecule (expected LE)	HAC	
2 (0.25)	10 (0.25)	13	4.8
	11 (0.25)	13	4.8
	12 (0.25)	13	4.8
	13 (0.25)	11	10.8
	14 (0.25)	7	56.2
	15 (0.25)	19	0.4
3 (0.25)	16 (0.25)	15	1.6
	17 (0.25)	15	1.6
4 (0.29)	18 (0.29)	9	12.4
	19 (0.29)	10	7.6
5 (0.31)	20 (0.31)	17	0.1
	21 (0.31)	14	0.7
6 (0.21)	22 (0.21)	12	12.7
	23 (0.22)	12	12.7
7 (0.30)	24 (0.30)	9	10.0
	25 (0.30)	15	0.5
8 (0.13)	26 (0.13)	10	119.3
	27 (0.13)	14	51.0
	28 (0.13)	16	33.3
	29 (0.13)	15	41.2
9 (0.20)	30 (0.20)	15	6.6
	31 (0.20)	17	3.4

^aThe LE was assumed to be conserved from the fragment to the inhibitor.⁸ HAC: heavy atom count.

have been published.^{11,12,41} In the first study, an inhibitor of the AmpC β -lactamase was deconstructed into three fragments with an apparent K_I of 40, 19, and 9 mM.¹¹ None of the fragments recapitulates the position of the inhibitor, whereas a more complex fragment containing two of the three functional groups of the lead ($K_D = 5$ mM) was shown to recapitulate the orientation of the lead. This work suggested that the fragment can interact as the lead only if a certain proportion of binding determinants is present. In another study,¹² all fragments retained the position of the lead. Interestingly, the K_I was shown to be <0.5 mM. In the study of Stout et al., all the fragments of *Escherichia coli* thymidylate-synthase display considerable fidelity of binding mode and interactions compared to the substrate.⁴¹ However, no information is available about the binding affinity of the fragments. Hence, even if some of the results are opposite, these studies may all suggest that a fragment will be able to retain its position in the lead if the determinants for the interaction are strong enough or the number of key determinants for the interaction are enough represented (the fragment exhibits a high group efficiency in the inhibitor).⁴⁰

Conclusion

In conclusion, the study we report here shows that the dissection of inhibitors is an interesting approach to select the best substructures in terms of binding efficiencies. In the case of Bcl-x_L, the best fragments resulting from the nine inhibitors are the diphenyl (10, 30), the naphthalene (22, 23), the benzophenone (31), the tetrahydroquinoline (26), and the indole (24). Our observations about the ligand efficiencies of the fragments confirm that, in order to design an inhibitor that respects the basic bioavailability and solubility constraints, it would be of great interest to evaluate each part of the molecule in terms of group efficiency to optimize each modification of the lead molecule. The results also show that the relation

between the complexity of the molecule and its binding properties is far from being obvious and indicates that the complexity of the fragment does not guarantee the conservation of the binding mode. Finally, the study reported here shows that the fragments not included in leads will interact with their preferred binding site, which can be different from the site they occupy when they are included in the larger molecule and illustrates the nonadditivity of fragments in protein–ligand binding. An interesting point would be to compare our NMR results with crystals structures of the Bcl-x_L/fragment complexes.

Materials and Methods

Protein Production and Purification. Human Bcl-x_L containing deletions in the C-terminus ($\Delta 197$ –233) and the internal loop between helix $\alpha 1$ and helix $\alpha 2$ ($\Delta 45$ –84) was expressed as a 6xHis-tagged protein in *Escherichia coli* strain BL21 (DE3). For NMR studies, cultures were grown to log phase at 37 °C in M9 medium supplemented with ¹⁵NH₄Cl as the sole nitrogen source to produce uniformly ¹⁵N-labeled proteins. Bcl-x_L synthesis was induced with 0.5 mM isopropyl β -D-1-thiogalactopyranoside for 2 h. Fractionally deuterated ¹⁵N–¹³C labeled Bcl-x_L was prepared by growing bacterial cells in M9 medium prepared with 75% (v/v) D₂O and using ¹⁵NH₄Cl and ¹³C-glucose as sole nitrogen and carbon sources. The 6xHis-tagged Bcl-x_L was purified in one step by Ni²⁺-affinity chromatography. NMR samples contained 0.1–0.5 mM Bcl-x_L protein in 90% H₂O/10% D₂O, 25 mM sodium phosphate (pH 7.0), 0.5 mM ethylenediaminetetraacetic acid (EDTA), and 3 mM dithiothreitol.

Organic Fragments. The fragments were obtained from Sigma-Aldrich or Acros and used without further purification. Aqueous solubility was checked for all fragments by recording 1D ¹H NMR and WaterLOGSY spectra.^{30,31} The 100 mM stock solutions of the library compounds were prepared in DMSO-*d*₆ and conserved at –20 °C. 1D ¹H NMR spectra were recorded to verify that no degradation occurs over 3 months.

NMR. NMR spectra were acquired with a Varian Inova 600 MHz NMR spectrometer, equipped with a standard 5 mm triple-resonance inverse probe with a *z*-axis field gradient, actively shielded, and with an autosampler robot.

Backbone Resonance Assignment of Bcl-x_L. NMR samples contained 0.5 mM of uniformly ¹⁵N/¹³C/50% ²H labeled Bcl-x_L protein in 90% H₂O/10% D₂O, 25 mM sodium phosphate (pH 7.0), 0.5 mM EDTA, and 3 mM dithiothreitol. The following experiments from the Varian Protein Pack were recorded at 28 °C for backbone ¹H^N and ¹⁵N resonance assignments: HNCA, HN(CO)CA, HNCACB. A ¹⁵N-HSQC spectrum was collected before and after each 3D experiment to check the protein stability. A 3D ¹H–¹⁵N NOESY-HSQC experiment was also recorded with a mixing time of 150 ms. All NMR spectra were processed with NMRPIPE software⁴² and analyzed using NMRView.⁴³

Binding Test and STD Measurements. Binding test was achieved at 20 °C using 1D STD³² and WaterLOGSY experiments with 1200 and 600 scans, respectively.^{30,31} The parameters used were the same as previously described.⁴⁴ Protein and fragment concentrations were set to 20 and 600 μ M, respectively. For quantitative analyses of STD spectra, the STD amplification factors f_{STD} were derived from the equation

$$f_{STD} = \frac{I_{STD}[L]_{tot}}{I_0 [P]_{tot}}$$

where I_{STD} and I_0 are peak integrals in the STD and 1D experiments, respectively, and $[L]_{tot}$ and $[P]_{tot}$ are the total concentrations of the ligand and protein, respectively. The 1D (1600 scans) and STD (3200 scans) experiments were performed under the same experimental conditions (spin lock, interscan delays), and parameters for the STD experiments (saturation

frequency, saturation time) were identical for all samples. STD signals were measured for aromatic protons. To easily compare the fragments, the STD factors have been scaled, using 100 for the strongest STD factor measured.

Binding Site Assessment. All NMR samples contained 80 μ M of uniformly 15 N-labeled Bcl-x_L protein and 0.5–2 mM of ligand (depending on solubility and affinity for the protein) in 90% H₂O/10% D₂O, 25 mM sodium phosphate (pH 7.0), 0.5 mM EDTA, and 3 mM dithiothreitol. Control ID 1 H spectra preceded all experiments to assess the purity and stability of the fragments. All NMR spectra were processed with the Varian VnmrJ software. Binding site was assessed at 28 °C using HSQC spectra with 64 t_1 increments. The HSQC spectra were processed with NMRPIPE software⁴² and analyzed using NMRView.⁴³

Binding Constant Measurement. The binding constant of **10** was determined by monitoring the changes in chemical shifts upon addition of increasing amounts of fragment. Protein concentration was set to 180 μ M and ligand concentration ranged from 0 to 4 mM. 15 N HSQC spectra were recorded at 28 °C with 48 scans and 64 t_1 increments. The HSQC spectra were processed with NMRPIPE software⁴² and analyzed using NMRView.⁴³

Docking. The fragment structures were generated and minimized with the SYBYL program (SYBYL-X 1.0, 2009). The fragments were docked in the 3D structure of the Bcl-x_L protein (PDB code 1YSG, Bcl-x_L in complex with “structure–activity relationship (SAR) by NMR” ligands) after removing the original ligands from the BH3 binding pocket. AutoDock 4.01⁴⁵ with the AutoDockTools graphical interface was used to simulate 50 different binding conformations for each fragment. Grid maps were generated with 0.375 Å spacing and set to encompass the residues perturbed upon fragment addition. The docking calculations were then performed using the Lamarckian genetic algorithm (LGA) for ligand conformational searching. The population size was set to 150, and the number of energy evaluations was 2 500 000.

Acknowledgment. S.B. is financially supported by a studentship from Ministère de la Recherche, France. The plasmid for the Bcl-x_L protein was kindly provided by Prof. Mingjie Zhang (Hong Kong University of Science and Technology).

Supporting Information Available: Figure showing the chemical shift changes observed on the protein spectrum plotted as a function of ligand concentration for the measurement of the dissociation constant of the **10**–Bcl-x_L interaction. This material is available free of charge via the Internet at <http://pubs.acs.org>.

References

- Hajduk, P. J.; Greer, J. A decade of fragment-based drug design: strategic advances and lessons learned. *Nat. Rev. Drug Discovery* **2007**, *6*, 211–219.
- Shuker, S. B.; Hajduk, P. J.; Meadows, R. P.; Fesik, S. W. Discovering high-affinity ligands for proteins: SAR by NMR. *Science* **1996**, *274*, 1531–1534.
- Rees, D. C.; Congreve, M.; Murray, C. W.; Carr, R. Fragment-based lead discovery. *Nat. Rev. Drug Discovery* **2004**, *3*, 660–672.
- Congreve, M.; Chessari, G.; Tisi, D.; Woodhead, A. J. Recent developments in fragment-based drug discovery. *J. Med. Chem.* **2008**, *51*, 3661–3680.
- Erlanson, D. A.; McDowell, R. S.; O'Brien, T. Fragment-based drug discovery. *J. Med. Chem.* **2004**, *47*, 3463–3482.
- Erlanson, D. A. Fragment-based lead discovery: a chemical update. *Curr. Opin. Biotechnol.* **2006**, *17*, 643–652.
- Hopkins, A. L.; Groom, C. R.; Alex, A. Ligand efficiency: a useful metric for lead selection. *Drug Discovery Today* **2004**, *9*, 430–431.
- Hajduk, P. J. Fragment-based drug design: how big is too big? *J. Med. Chem.* **2006**, *49*, 6972–6976.
- Murray, C. W.; Verdonk, M. L. The consequences of translational and rotational entropy lost by small molecules on binding to proteins. *J. Comput.-Aided Mol. Des.* **2002**, *16*, 741–753.
- Ciulli, A.; Williams, G.; Smith, A. G.; Blundell, T. L.; Abell, C. Probing hot spots at protein–ligand binding sites: a fragment-based approach using biophysical methods. *J. Med. Chem.* **2006**, *49*, 4992–5000.
- Babaoglu, K.; Shoichet, B. K. Deconstructing fragment-based inhibitor discovery. *Nat. Chem. Biol.* **2006**, *2*, 720–723.
- Andersen, O. A.; Nathubhai, A.; Dixon, M. J.; Eggleston, I. M.; van Aalten, D. M. Structure-based dissection of the natural product cyclopentapeptide chitinase inhibitor argifin. *Chem. Biol.* **2008**, *15*, 295–301.
- Muchmore, S. W.; Sattler, M.; Liang, H.; Meadows, R. P.; Harlan, J. E.; Yoon, H. S.; Nettlesheim, D.; Chang, B. S.; Thompson, C. B.; Wong, S. L.; Ng, S. L.; Fesik, S. W. X-ray and NMR structure of human Bcl-x_L, an inhibitor of programmed cell death. *Nature* **1996**, *381*, 335–341.
- Adams, J. M.; Cory, S. The Bcl-2 apoptotic switch in cancer development and therapy. *Oncogene* **2007**, *26*, 1324–1337.
- Yin, X. M.; Oltvai, Z. N.; Korsmeyer, S. J. BH1 and BH2 domains of Bcl-2 are required for inhibition of apoptosis and heterodimerization with Bax. *Nature* **1994**, *369*, 321–323.
- Oltvai, Z. N.; Korsmeyer, S. J. Checkpoints of dueling dimers foil death wishes. *Cell* **1994**, *79*, 189–192.
- Kang, M. H.; Reynolds, C. P. Bcl-2 inhibitors: targeting mitochondrial apoptotic pathways in cancer therapy. *Clin. Cancer Res.* **2009**, *15*, 1126–1132.
- Sattler, M.; Liang, H.; Nettlesheim, D.; Meadows, R. P.; Harlan, J. E.; Eberstadt, M.; Yoon, H. S.; Shuker, S. B.; Chang, B. S.; Minn, A. J.; Thompson, C. B.; Fesik, S. W. Structure of Bcl-x_L–Bak peptide complex: recognition between regulators of apoptosis. *Science* **1997**, *275*, 983–986.
- Lugovskoy, A. A.; Degterev, A. I.; Fahmy, A. F.; Zhou, P.; Gross, J. D.; Yuan, J.; Wagner, G. A novel approach for characterizing protein ligand complexes: molecular basis for specificity of small-molecule Bcl-2 inhibitors. *J. Am. Chem. Soc.* **2002**, *124*, 1234–1240.
- Mohammad, R. M.; Goustin, A. S.; Aboukameel, A.; Chen, B.; Banerjee, S.; Wang, G.; Nikolovska-Coleska, Z.; Wang, S.; Al-Katib, A. Preclinical studies of TW-37, a new nonpeptidic small-molecule inhibitor of Bcl-2, in diffuse large cell lymphoma xenograft model reveal drug action on both Bcl-2 and Mcl-1. *Clin. Cancer Res.* **2007**, *13*, 2226–2235.
- Nguyen, M.; Marcellus, R. C.; Roulston, A.; Watson, M.; Serfass, L.; Murthy Madiraju, S. R.; Goulet, D.; Viallet, J.; Belec, L.; Billot, X.; Acoca, S.; Purisima, E.; Wiegman, A.; Cluse, L.; Johnstone, R. W.; Beauparlant, P.; Shore, G. C. Small molecule obatoclax (GX15-070) antagonizes MCL-1 and overcomes MCL-1-mediated resistance to apoptosis. *Proc. Natl. Acad. Sci. U.S.A.* **2007**, *104*, 19512–19517.
- Oltersdorf, T.; Elmore, S. W.; Shoemaker, A. R.; Armstrong, R. C.; Augeri, D. J.; Belli, B. A.; Bruncko, M.; Deckwerth, T. L.; Dinges, J.; Hajduk, P. J.; Joseph, M. K.; Kitada, S.; Korsmeyer, S. J.; Kunzer, A. R.; Letai, A.; Li, C.; Mitten, M. J.; Nettlesheim, D. G.; Ng, S.; Nimmer, P. M.; O'Connor, J. M.; Oleksijew, A.; Petros, A. M.; Reed, J. C.; Shen, W.; Tahir, S. K.; Thompson, C. B.; Tomaselli, K. J.; Wang, B.; Wendt, M. D.; Zhang, H.; Fesik, S. W.; Rosenberg, S. H. An inhibitor of Bcl-2 family proteins induces regression of solid tumours. *Nature* **2005**, *435*, 677–681.
- Prakesch, M.; Denisov, A. Y.; Naim, M.; Gehring, K.; Arya, P. The discovery of small molecule chemical probes of Bcl-X(L) and Mcl-1. *Bioorg. Med. Chem.* **2008**, *16*, 7443–7449.
- Qiu, J.; Levin, L. R.; Buck, J.; Reidenberg, M. M. Different pathways of cell killing by gossypol enantiomers. *Exp. Biol. Med. (Maywood, N.J., U. S.)* **2002**, *227*, 398–401.
- Rega, M. F.; Leone, M.; Jung, D.; Cotton, N. J.; Stebbins, J. L.; Pellecchia, M. Structure-based discovery of a new class of Bcl-x_L antagonists. *Bioorg. Chem.* **2007**, *35*, 344–353.
- Schwartz, P. S.; Manion, M. K.; Emerson, C. B.; Fry, J. S.; Schulz, C. M.; Sweet, I. R.; Hockenbery, D. M. 2-Methoxy antimycin reveals a unique mechanism for Bcl-x(L) inhibition. *Mol. Cancer Ther.* **2007**, *6*, 2073–2080.
- Tse, C.; Shoemaker, A. R.; Adickes, J.; Anderson, M. G.; Chen, J.; Jin, S.; Johnson, E. F.; Marsh, K. C.; Mitten, M. J.; Nimmer, P.; Roberts, L.; Tahir, S. K.; Xiao, Y.; Yang, X.; Zhang, H.; Fesik, S.; Rosenberg, S. H.; Elmore, S. W. ABT-263: a potent and orally bioavailable Bcl-2 family inhibitor. *Cancer Res.* **2008**, *68*, 3421–3428.
- Wang, J. L.; Liu, D.; Zhang, Z. J.; Shan, S.; Han, X.; Srinivasula, S. M.; Croce, C. M.; Alnemri, E. S.; Huang, Z. Structure-based discovery of an organic compound that binds Bcl-2 protein and induces apoptosis of tumor cells. *Proc. Natl. Acad. Sci. U.S.A.* **2000**, *97*, 7124–7129.

- (29) Leone, M.; Zhai, D.; Sareth, S.; Kitada, S.; Reed, J. C.; Pellecchia, M. Cancer prevention by tea polyphenols is linked to their direct inhibition of antiapoptotic Bcl-2-family proteins. *Cancer Res.* **2003**, *63*, 8118–8121.
- (30) Dalvit, C.; Fogliatto, G.; Stewart, A.; Veronesi, M.; Stockman, B. WaterLOGSY as a method for primary NMR screening: practical aspects and range of applicability. *J. Biomol. NMR* **2001**, *21*, 349–359.
- (31) Dalvit, C.; Pevarello, P.; Tato, M.; Veronesi, M.; Vulpetti, A.; Sundstrom, M. Identification of compounds with binding affinity to proteins via magnetization transfer from bulk water. *J. Biomol. NMR* **2000**, *18*, 65–68.
- (32) Mayer, M.; Meyer, B. Characterization of ligand binding by saturation transfer difference NMR spectroscopy. *Angew. Chem., Int. Ed.* **1999**, *38*, 1784–1788.
- (33) Meinecke, R.; Meyer, B. Determination of the binding specificity of an integral membrane protein by saturation transfer difference NMR: RGD peptide ligands binding to integrin α IIb β 3. *J. Med. Chem.* **2001**, *44*, 3059–3065.
- (34) Petros, A. M.; Dinges, J.; Augeri, D. J.; Baumeister, S. A.; Betebenner, D. A.; Bures, M. G.; Elmore, S. W.; Hajduk, P. J.; Joseph, M. K.; Landis, S. K.; Nettekheim, D. G.; Rosenberg, S. H.; Shen, W.; Thomas, S.; Wang, X.; Zanze, I.; Zhang, H.; Fesik, S. W. Discovery of a potent inhibitor of the antiapoptotic protein Bcl-xL from NMR and parallel synthesis. *J. Med. Chem.* **2006**, *49*, 656–663.
- (35) Congreve, M.; Carr, R.; Murray, C.; Jhoti, H. A “rule of three” for fragment-based lead discovery? *Drug Discovery Today* **2003**, *8*, 876–877.
- (36) Lee, E. F.; Czabotar, P. E.; Smith, B. J.; Deshayes, K.; Zobel, K.; Colman, P. M.; Fairlie, W. D. Crystal structure of ABT-737 complexed with Bcl-xL: implications for selectivity of antagonists of the Bcl-2 family. *Cell Death Differ.* **2007**, *14*, 1711–1713.
- (37) Becattini, B.; Kitada, S.; Leone, M.; Monosov, E.; Chandler, S.; Zhai, D.; Kipps, T. J.; Reed, J. C.; Pellecchia, M. Rational design and real time, in-cell detection of the proapoptotic activity of a novel compound targeting Bcl-X(L). *Chem. Biol.* **2004**, *11*, 389–395.
- (38) Kitada, S.; Leone, M.; Sareth, S.; Zhai, D.; Reed, J. C.; Pellecchia, M. Discovery, characterization, and structure–activity relationships studies of proapoptotic polyphenols targeting B-cell lymphocyte/leukemia-2 proteins. *J. Med. Chem.* **2003**, *46*, 4259–4264.
- (39) Wang, G.; Nikolovska-Coleska, Z.; Yang, C. Y.; Wang, R.; Tang, G.; Guo, J.; Shangary, S.; Qiu, S.; Gao, W.; Yang, D.; Meagher, J.; Stuckey, J.; Krajewski, K.; Jiang, S.; Roller, P. P.; Abaan, H. O.; Tomita, Y.; Wang, S. Structure-based design of potent small-molecule inhibitors of anti-apoptotic Bcl-2 proteins. *J. Med. Chem.* **2006**, *49*, 6139–6142.
- (40) Verdonk, M. L.; Rees, D. C. Group efficiency: a guideline for hits-to-leads chemistry. *ChemMedChem* **2008**, *3*, 1179–1180.
- (41) Stout, T. J.; Sage, C. R.; Stroud, R. M. The additivity of substrate fragments in enzyme–ligand binding. *Structure* **1998**, *6*, 839–848.
- (42) Delaglio, F.; Grzesiek, S.; Vuister, G. W.; Zhu, G.; Pfeifer, J.; Bax, A. NMRPipe: a multidimensional spectral processing system based on UNIX pipes. *J. Biomol. NMR* **1995**, *6*, 277–293.
- (43) Johnson, B. A.; Blevins, R. A. NMR View, a computer-program for the visualization and analysis of NMR data. *J. Biomol. NMR* **1994**, *4*, 603–614.
- (44) Bretonnet, A. S.; Jochum, A.; Walker, O.; Krimm, I.; Goekjian, P.; Marcillat, O.; Lancelin, J. M. NMR screening applied to the fragment-based generation of inhibitors of creatine kinase exploiting a new interaction proximate to the ATP binding site. *J. Med. Chem.* **2007**, *50*, 1865–1875.
- (45) Morris, G. M.; Huey, R.; Olson, A. J. Using AutoDock for Ligand–Receptor Docking. In *Current Protocols in Bioinformatics*; Wiley: Somerset, NJ, 2008; Chapter 8, Unit 8, p 14.